Available online at www.sciencedirect.com
SCIENCE DIRECT®
Journal of Catalysis 230 (2005) 86–97
JOURNAL OF CATALYSIS
www.elsevier.com/locate/jcat

Hydrogen-assisted 1,2-dichloroethane dechlorination catalyzed by Pt–Sn/SiO_2 catalysts of different preparations

William D. Rhodes [a,1], József L. Margitfalvi [b], Irina Borbáth [b], Károly Lázár [c], Vladimir I. Kovalchuk [a], Julie L. d'Itri [a,*]

[a] *Department of Chemical Engineering, University of Pittsburgh, Pittsburgh, PA 15261, USA*
[b] *Institute of Surface Chemistry and Catalysis, Chemical Research Center, Hungarian Academy of Sciences, Budapest, PO Box 17, H-1525, Hungary*
[c] *Institute of Isotopes, Chemical Research Center, Hungarian Academy of Sciences, Budapest, PO Box 77, H-1525, Hungary*

Received 5 August 2004; revised 10 November 2004; accepted 15 November 2004

Abstract

The effect of Sn content on the activity and selectivity for hydrogen-assisted 1,2-dichloroethane dechlorination catalyzed by Pt–Sn/SiO_2 catalysts prepared via controlled surface reaction (CSR) has been investigated. For catalysts with a Pt/Sn atomic ratio greater than unity, the major and minor reaction products are ethane and ethyl chloride, respectively. As the ratio is decreased, the ethylene selectivity increases from zero to almost 90% at a Pt/Sn ratio of 0.8; concomitantly, the activity expressed as a turnover frequency decreases by a factor of 5. Each Sn-rich catalyst (Pt/Sn $\leqslant 1$) exhibits a transient period (5–110 h) during which sites for olefin formation are created. In situ ^{119}Sn Mössbauer spectroscopic investigations of the Pt–Sn/SiO_2 catalyst with a Pt/Sn atomic ratio of 0.5 showed that all Sn in the reduced sample is incorporated into Sn-rich and Pt-rich Pt–Sn alloys; the latter phase predominates. In contrast, a reduced Pt–Sn/SiO_2 catalyst with the same overall composition but prepared by co-impregnation contains Sn^{2+} and Sn^{4+} ions in addition to the metallic Sn that is incorporated into Pt–Sn alloys. The CSR catalyst exhibits a higher initial selectivity toward ethylene than the co-impregnated catalyst (66 and 5%, respectively, after reduction at 623 K), whereas the steady-state ethylene selectivity is higher for the co-impregnated sample (91 and 75%, respectively). These results are discussed in terms of the different genesis and microstructures of the CSR and co-impregnated Pt–Sn/SiO_2 catalysts.

Keywords: Hydrogen-assisted dechlorination; 1,2-Dichloroethane; Ethylene; SiO_2; Platinum; Tin; Pt–Sn/SiO_2; Controlled surface reaction; Mössbauer spectroscopy

---

1. Introduction

Additives such as Sn play an essential role in controlling the activity, selectivity, and stability of many noble metals used to catalyze reactions such as hydrocarbon reforming [1,2], oxidation of methanol [3,4] and CO [5–7], oxidative dehydrogenation of light alkanes [8–11], selective catalytic reduction of NO_x with hydrocarbons [12,13], olefin hydroformylation [14], and selective hydrogenation of nitriles [15] and α,β-unsaturated aldehydes [16–20]. It has also been shown that the addition of Sn to Pt improves the catalytic performance for hydrogen-assisted dechlorination reactions such as 1,2-dichloroethane conversion to ethylene [6,21] and 1,2,3-trichloropropane conversion to propylene and/or allyl chloride [22].

Although many investigations have been conducted [5,17,19,23–33], the mechanism by which Sn improves the performance of Group VIII noble metals in various reactions is still a matter of debate. Indeed, the Pt–Sn system is complex: five intermetallic compounds are thermodynamically stable [34]. Moreover, different Sn(II) and Sn(IV) ion-containing species may form [6,35–40]. Thus, it is extremely challenging to determine the impact of each particu-

---

[*] Corresponding author. Fax: +1 412 624 9639.
E-mail address: jditri@pitt.edu (J.L. d'Itri).

[1] Present address: Westinghouse Savannah River Company, Bldg 773A, Aiken, SC 29808, USA.

0021-9517/$ – see front matter © 2004 Elsevier Inc. All rights reserved.
doi:10.1016/j.jcat.2004.11.019

lar species on the overall catalyst performance, especially because the type of surface species present under conditions of real catalysis depends on the reaction conditions. Moreover, bimetallic catalysts prepared by sequential or co-impregnation of the support with a solution of inorganic metal salts are plagued by inhomogeneity [36,41].

In a previous investigation kinetics results were correlated with Mössbauer studies of impregnated Pt–Sn/SiO_2 catalysts [21]. It was concluded that the Sn-rich Pt–Sn alloy particles are responsible for ethylene formation in hydrogen-assisted 1,2-dichloroethane dechlorination, whereas Pt and Pt-rich Pt–Sn species catalyze the formation of ethane. However, the role of ionic Sn in the Pt–Sn/SiO_2 catalysts for the hydrogen-assisted conversion of vicinal chlorocarbons has yet to be addressed. It has been suggested that ionic Sn species modify significantly the catalytic performance of Pt in the reactions of hydrocarbon hydroconversion [42], α,β-unsaturated aldehyde-selective hydrogenation [19,25], and low-temperature CO oxidation [5,7,19,43].

To understand the role of ionic Sn species in Pt–Sn-catalyzed dechlorination reactions, two different preparation procedures were used in the present investigation to vary the interaction between Pt and Sn: conventional co-impregnation and an organometallic method utilizing a controlled surface reaction (CSR) between hydrogen adsorbed to silica-supported Pt and tetraethyl tin [19,44–47]. In contrast to co-impregnation methods, organometallic methods employing CSR ensure the formation of exclusively bimetallic moieties on the surface of the support [19,44,47,48]. The Pt–Sn interactions in the Pt–Sn/SiO_2 catalysts with the same overall composition but prepared via different procedures were characterized by ^{119}Sn Mössbauer spectroscopy. The results were linked to the catalytic performance in hydrogen-assisted 1,2-dichloroethane dechlorination.

2. Experimental

2.1. Catalyst preparation and routine characterization

Davisil-grade 645 (60–100 mesh, surface area 300 $m^2\,g^{-1}$, average pore diameter 150 Å, pore volume 1.15 $cm^3\,g^{-1}$) silica gel (Aldrich, 99+%) was used as a support. Two monometallic Pt/SiO_2 catalysts with metal loading of 0.4 and 0.7% (Galbraith Laboratories) were prepared by pore volume impregnation of the support with aqueous solutions of $H_2PtCl_6 \cdot 6H_2O$ (Alfa, 99.9%). The slurry was equilibrated overnight before drying at ambient temperature and pressure for 72 h, followed by further drying at 373 K for 2 h under vacuum (∼ 5 Torr).

A bimetallic Pt–Sn/SiO_2 catalyst with a Pt/Sn atomic ratio of 0.5 (sample T-0.5, Table 1) was prepared by pore volume co-impregnation of the silica support with a solution of $H_2PtCl_6 \cdot 6H_2O$ (Alfa, 99.9%) and $SnCl_2 \cdot 2H_2O$ (Aldrich, 98%) in 1 N aqueous HCl. The drying procedure was the same as that used for the Pt/SiO_2 catalysts. The Pt and Sn loadings in the reduced catalyst were 0.4 and 0.5%, respectively (Galbraith Laboratories, Table 1). More details of the co-impregnation preparation procedure can be found elsewhere [21].

The 0.4% Pt/SiO_2 and 0.7% Pt/SiO_2 catalysts were used as the starting materials for the preparation of the Pt–Sn/SiO_2 catalysts by means of CSR (N-series, Table 1). The Pt/SiO_2 catalyst was reduced by flowing H_2 (30 ml min^{-1}) at 573 K for 1 h. After reduction the catalyst was cooled to room temperature in the H_2 flow and then purged with Ar (30 ml min^{-1}) for 30 min to remove the physisorbed H_2. Next, the catalyst was transferred into a glass reactor without exposure to air and slurried with deoxygenated benzene in an Ar atmosphere. The slurry was heated from room temperature to 323 K. At 323 K the Sn anchoring reaction was started by injecting tetraethyl tin into the slurry:

$$PtH_{ads} + Sn(C_2H_5)_4 \rightarrow Pt\text{–}Sn(C_2H_5)_{4-x} + xC_2H_6. \qquad (1)$$

The extent of reaction (1) was determined from the change in concentration of C_2H_6 both in the gas phase and in the slurry and from the change in the $Sn(C_2H_5)_4$ concentration in the slurry measured with a gas chromatograph (GC). The GC was equipped with a 3-m Al_2O_3 packed column operated at 373 K to quantify C_2H_6 and a 1.5-m SiO_2/10% Silicon 410 packed column operated at 433 K to quantify $Sn(C_2H_5)_4$. When reaction (1) reached completion, the catalyst was washed at 323 K four times with benzene and twice with n-hexane. Then, the catalyst was dried in vacuum (5 Torr) for 1 h at the same temperature. This procedure was used to prepare the catalyst with a Pt/Sn ratio of 2.5 (N-2.5).

The CSR catalyst N-1.7 was prepared with the use of H_2 as the reaction medium instead of Ar to increase the amount of anchored Sn [45]. For the preparation of the N-1.0, N-0.6, and N-0.5 catalysts, the Sn anchoring was started in H_2; 150 min after the beginning of the anchoring procedure, the H_2 was replaced with Ar. Then, a small amount of O_2 (20 cm^3/g_{cat}) was added to the reactor, and the Sn anchoring was continued. Previous research has shown that O_2 addition substantially increases the amount of Sn anchored [45]. For the N-0.8 catalyst two sequential Sn anchorings were performed. The first anchoring by the same procedure as applied for the preparation of the N-1.0, N-0.6, and N-0.5 catalysts with subsequent reduction at 623 K resulted in a Pt/Sn atomic ratio of 0.9. The second anchoring was also conducted in H_2 but without the addition of O_2, and it resulted in a final Pt/Sn ratio of 0.8. The Sn anchoring (reaction (1)) was conducted for 3–8 h. To increase the amount of anchored Sn, a sufficiently longer reaction time was used compared with earlier work [44,49,50].

The decomposition of the Pt–$Sn(C_2H_5)_{4-x}$ surface complex was conducted in flowing H_2 (30 ml min^{-1}) during heating from 298 to 623 K at a rate of 5 K min^{-1} with 2 g of the catalyst in the reactor:

$$Pt\text{–}Sn(C_2H_5)_{4-x} + (4-x)/2H_2 \rightarrow Pt\text{–}Sn + (4-x)C_2H_6 \qquad (2)$$

Table 1
Results of routine characterization of the Pt/SiO_2 and $Pt–Sn/SiO_2$ catalysts

Catalyst[a]	Pt loading[b] (wt%)	Sn loading (wt%)	Pt/Sn atomic ratio	CO/Pt[e] (%)	Cl content[b,d] (wt%)	
					Before reaction	After reaction
Pt-0.4	0.4	0	∞	61	n.d.	n.d.
Pt-0.7	0.7	0	∞	58	n.d.	n.d.
N-2.5	0.7	0.15[c]	2.5	17	n.d.	n.d.
N-1.7	0.7	0.25[c]	1.7	18	n.d.	n.d.
N-1.0	0.7	0.45[c]	1.0	9	n.d.	n.d.
N-0.8	0.7	0.55[c]	0.8	5	n.d.	n.d.
N-0.6	0.7	0.7[c]	0.6	11	n.d.	n.d.
N-0.5	0.4	0.5[c]	0.5	18	0.1	0.1
T-0.5	0.4	0.5[b]	0.5	16	0.1	0.4

[a] T, catalyst prepared by coimpregnation; N, catalyst prepared by CSR.

[b] Galbraith Laboratories, Inc.

[c] Atomic absorption spectroscopy.

[d] n.d., chlorine content was not determined.

[e] Based on irreversible CO uptake, $CO/Pt_{total} \times 100\%$.

and/or

$$Pt–Sn(C_2H_5)_{4-x} \rightarrow Pt–Sn + (4-x)/2C_2H_6 + (4-x)/2C_2H_4. \quad (3)$$

The decomposition products (C_2H_6 and C_2H_4) were quantified by a GC equipped with a 3-m Al_2O_3 packed column. After decomposition the Sn loading in the catalysts was determined by atomic absorption spectroscopy.

Carbon monoxide chemisorption measurements were conducted at 308 K within a CO pressure range of 100–500 Torr with a volumetric sorption analyzer (Micromeritics ASAP 2010). Prior to the measurement, the catalyst was reduced in flowing H_2 (30 ml min^{-1}) at 573 K for 2 h followed by reduction at 623 K for 1 h. Then, the system was evacuated at 623 K and cooled to the measurement temperature. The adsorbate/metal ratios were determined from the amount of irreversibly adsorbed CO (Table 1); the adsorption stoichiometry was assumed to be 1 [51]. All chemisorption measurements were conducted at least twice, and the reproducibility was better than ±5%.

2.2. Hydrogen-assisted 1,2-dichloroethane dechlorination

The dechlorination of CH_2ClCH_2Cl was conducted at ambient pressure in a stainless-steel flow reaction system connected to a quartz microreactor (10 mm i.d.) in which the catalyst was supported on a quartz frit. The reactor zone containing the catalyst was heated by an electric furnace. The catalyst temperature was measured and controlled with an accuracy of ±1 K with a temperature controller (Omega model CN2011). The gaseous reactants were metered with mass flow controllers (Brooks, 5850E) and mixed before they were introduced into the reactor. The liquid CH_2ClCH_2Cl (Sigma–Aldrich, 99.8%) was maintained in a saturator at 273 ± 0.01 K with a recirculating cooling system (RTE-7/Digital 1, Thermo NESLAB) and metered into the reaction system via He carrier gas. Saturation was confirmed by varying the flow rate of He through the saturator and quantifying the CH_2ClCH_2Cl in the gas phase with a GC (Varian 3300 series).

The reactor effluent was analyzed by on-line GC and, when necessary, by GC/MS to identify the reaction products. The GC was equipped with a 3-m 60/80 Carbopack B/5% Fluorocol packed column (Supelco) and a flame ionization detector (FID) capable of detecting concentrations greater than 1 ppm for all chlorocarbons and hydrocarbons involved in this study. The on-line HP GC/MS system consisted of a HP 5890 Series II Plus GC equipped with a Fluorocol column connected to a HP 5972 series mass-selective detector. Hydrogen chloride, a reaction product, was detected by GC/MS but was not quantified.

Prior to reaction the catalyst was exposed to flowing He (Praxair, 99.999%, 30 ml min^{-1}) while heating from 303 to 403 K at a rate of 7 K min^{-1} and then held at 403 K for 60 min. Then, the gas stream was switched to a mixture of H_2 (Praxair, 99.999%, 10 ml min^{-1}) and He (50 ml min^{-1}). Next, the catalyst was heated from 403 K to the reduction temperature (493 or 623 K) for 30 min and held at this temperature for 90 min. Last, the catalyst was quickly cooled in He (50 ml min^{-1}) to the reaction temperature.

For a typical dechlorination reaction, 0.15 g of catalyst was used and the total flow of reactant mixture was 16 ml min^{-1}. The flow consisted of CH_2ClCH_2Cl (7300 ppm), H_2 (36,800 ppm), and He (balance). The reaction temperature was 473 K. The catalyst mass and reactant mixture flow rate were adjusted to maintain the conversion in a narrow range (0.5 to 1.1%) so that the selectivity patterns could be compared. The turnover frequency (TOF) values were calculated with the use of the fraction of exposed Pt atoms determined from CO chemisorption measurements. All kinetics experiments were conducted at least twice, and the reproducibility was better than ±5%.

2.3. Mössbauer spectroscopy

The ^{119}Sn Mössbauer spectra were recorded at 77 K in an in situ cell [52] with a pellet supported on a thin Be plate. The pellet was made from a powdered catalyst sample (ca. 0.7 g) by pressing the sample at 100 MPa for 3 min. Spectra were obtained for the as-prepared samples, for the samples after reduction in flowing H_2 at 493 K, and after a second reduction of the same sample at 623 K (2 h, 10 ml min^{-1}, ambient pressure for both reductions). The last spectrum for each sample was collected after exposure of the reduced catalyst to a flow of $CH_2Cl–CH_2Cl + H_2 + N_2$ (1:5:25, 13 ml min^{-1}, ambient pressure) at 473 K for 24 h. The exposure time was chosen to provide a quasi-steady-state catalyst performance for 1,2-dichloroethane dechlorination. The cell was sealed in the specific treatment gas after each step and cooled to the measurement temperature.

The constant acceleration Mössbauer spectra were collected with a KFKI spectrometer and a Ba $^{119m}SnO_3$ source (300 MBq). For fitting purposes a Lorentzian line shape for each peak was assumed, and no isomer shift parameters were initially constrained. Successive iterations were applied to obtain a better fit to the experimental data. The estimated accuracy of the positional parameters was 0.03 mm s^{-1}. The isomer shift values were determined relative to the value for SnO_2 (room temperature).

3. Results

3.1. Routine catalyst characterization

The CO/Pt ratio for the Pt-0.4 and Pt-0.7 catalysts was 61 and 58%, respectively (Table 1). For N-2.5, N-1.7, N-0.5, and T-0.5, the CO/Pt ratio was between 16 and 18%. The lowest CO/Pt ratio (5%) was observed for the N-0.8 catalyst; for the N-1.0 and N-0.6 samples it was approximately 10% (Table 1).

The N-0.5 and T-0.5 catalysts were analyzed for Cl. The residual Cl content was 0.1% for both samples after reduction at 493 K. Exposure of the N-0.5 sample to the $ClCH_2–CH_2Cl + H_2$ reaction mixture at 473 K for 65 h did not change the Cl concentration. However, the Cl concentration of the T-0.5 sample increased by a factor of 4 to 0.4% after 65 h on stream at 473 K (Table 1).

3.2. Kinetics experiments

The catalytic performance of supported Pt for the $CH_2Cl–CH_2Cl + H_2$ reaction is well documented [21,53], and thus the parent Pt/SiO_2 catalysts were not tested. According to the literature, the steady-state TOF of Pt/SiO_2 is in the range of 2×10^{-3} to 4×10^{-3} s^{-1}, depending on the metal loading [21,53]. A 0.5% Pt/SiO_2 catalyst deactivated during the first 20 h on stream, and the 1,2-dichloroethane conversion decreased by a factor of 2.5. At longer time on stream the deactivation was insignificant [53]. With a 1.8% Pt/SiO_2 catalyst the conversion decreased by almost one order of magnitude during the first 100 h on stream [21]. The different extent of deactivation accounts for the different steady-state TOFs of the 0.5% Pt/SiO_2 and 1.8% Pt/SiO_2 catalysts. Monometallic Pt catalysts do not catalyze hydrogen-assisted 1,2-dichloroethane dechlorination to form ethylene; ethane and monochloroethane are the only reaction products [21,53]. Monometallic Sn catalysts exhibit no activity in the reaction [21].

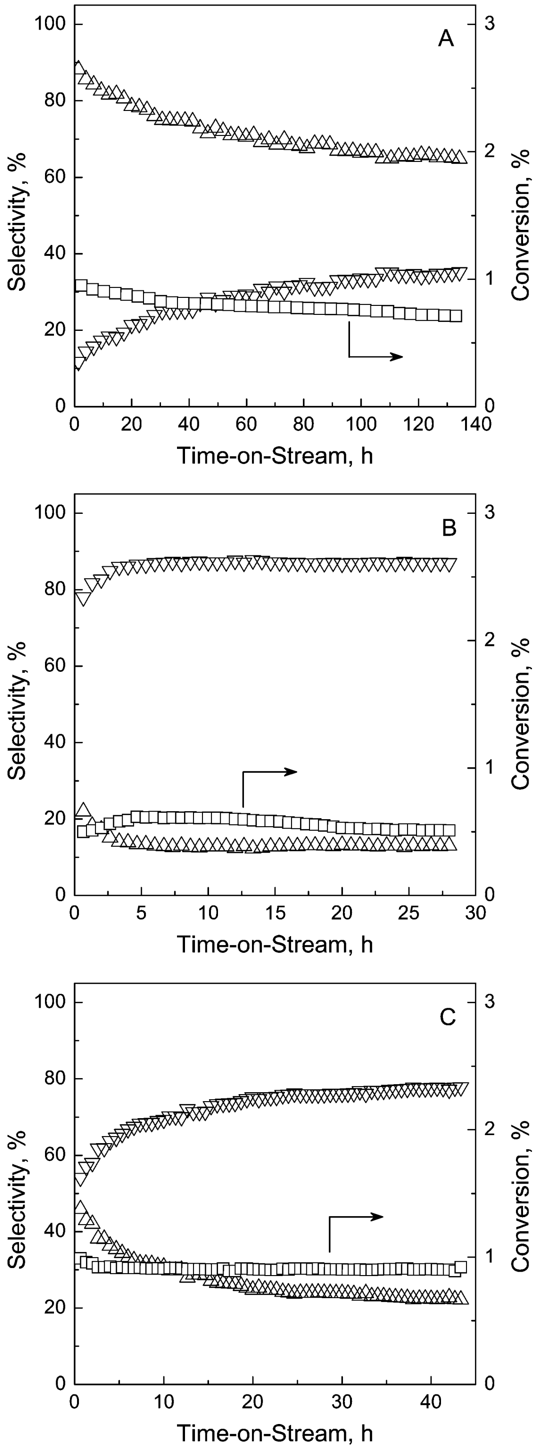

Fig. 1. Time on stream performance of the reduced at 493 K catalysts prepared by CSR: N-1.0 (A), N-0.8 (B), and N-0.6 (C). (△), ethane; (▽), ethylene; (☐), conversion.

With each bimetallic catalyst the conversion decreased during the first 0.7 h on stream; the total decrease during this

Table 2
1,2-Dichloroethane dechlorination catalyzed by Pt/SiO$_2$ and (Pt–Sn)/SiO$_2$

Catalyst	T_{red} (K)	TOS for SS[a]	Conversion[b] (%)	Initial selectivity[c,d] (mol%)		Steady state selectivity[d] (mol%)		TOF ($\times 10^4$ s^{-1})
				C_2H_4	C_2H_6	C_2H_4	C_2H_6	
Pt-0.5[e]	493	20	2.7	0	89	0	83	40.0
Pt-1.8[f]	493	85	1.4	0	91	0	89	23.0
N-2.5	493	3	0.9	0	96	0	96	16.8
N-1.7	493	4	1.1	0	96	0	97	15.8
N-1.0	493	110	0.7	10	90	36	64	10.5
N-0.8	493	5	0.5	79	21	87	13	12.9
N-0.6	493	30	0.9	52	48	78	22	8.4
N-0.5	493	12	0.6	66	34	85	15	7.6
N-0.5	623	10	0.6	66	34	75	25	7.6
T-0.5	493	64	0.7	11	89	88	12	9.1
T-0.5	623	35	0.7	5	95	91	9	8.8

[a] Time on stream to reach the steady-state catalyst performance when the change in conversion is less than 0.1% and the change in product selectivity is less than 1% for 5 h.

[b] At steady state.

[c] After 0.7 h of time on stream.

[d] Balanced by ethyl chloride.

[e] 0.5% Pt/SiO$_2$ [53].

[f] 1.8% Pt/SiO$_2$ [21].

time ranged from 42 to 81% (not shown). At longer times on stream the deactivation rate was 0–3% every 5 h. The highest deactivation was for the N-2.5 and N-1.7 catalysts—approximately 3% every 5 h. For the other bimetallic catalysts, there was essentially no deactivation with time on stream after the initial decrease (Figs. 1 and 2). The steady-state TOFs of the Pt–Sn/SiO$_2$ catalysts varied from 7.6×10^{-4} to 16.8×10^{-4} s^{-1}, depending on the Pt/Sn atomic ratio (Table 2). Specifically, the TOF gradually decreased as the Pt/Sn ratio decreased until it became essentially invariant at Pt/Sn atomic ratios equal to or less than 0.6 (Table 2).

Decreasing the Pt/Sn atomic ratio also resulted in an increase in the steady-state selectivity toward ethylene (Table 2). Monometallic Pt and Pt–Sn catalysts with higher Pt/Sn ratios (N-2.5 and N-1.7) yielded ethane (96–97%) and ethyl chloride (3–4%). At a Pt/Sn ratio of 1 (N-1.0), ethane was the major product (64%) and the balance was ethylene. For the N-0.8, N-0.6, and N-0.5 catalysts, the major product was ethylene (78–87%) and the balance was ethane. During the transient period the ethylene selectivity of the bimetallic catalysts with a Pt/Sn ratio less than or equal to 1 increased substantially at the expense of ethane (Figs. 1 and 2).

The time on stream performances of the catalysts with a Pt/Sn ratio of 0.5 prepared by co-impregnation (sample T-0.5) and by CSR (sample N-0.5) are compared in Fig. 2. The initial and steady-state product selectivities and the steady-state TOF values are shown in Table 2. At steady state both catalysts yielded ethylene as the major product and ethane as the minor product. However, the T-0.5 sample showed a significant improvement in selectivity toward ethylene with time on stream at the expense of ethane. Specifically, after reduction at 493 K the selectivity toward ethylene increased from 11 to 88% during 64 h on stream (Fig. 2A). For the N-0.5 sample the steady-state selectivity toward ethylene at the expense of ethane was reached during a shorter time pe-

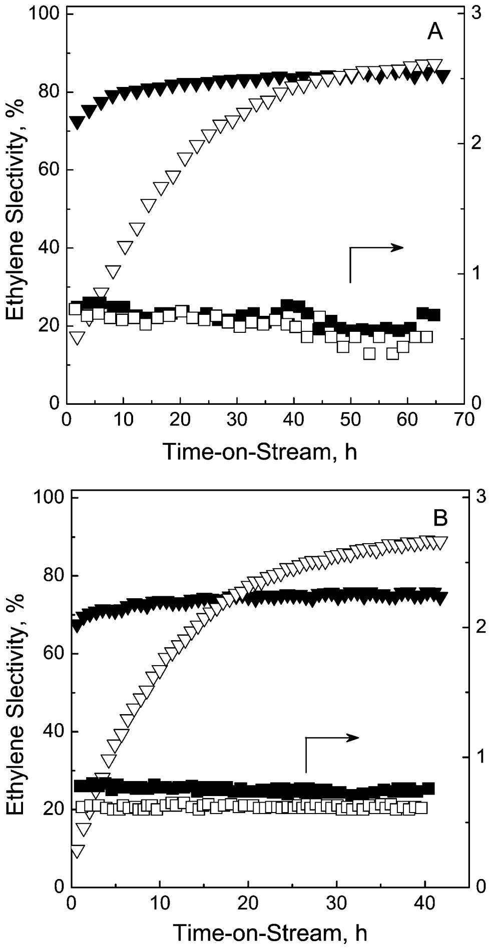

Fig. 2. Time on stream performance of the CSR (N-0.5) and impregnated (T-0.5) catalysts reduced at 493 K (A) and 623 K (B): (▽) and (▼), ethylene, for the T and N samples, respectively (balance is ethane); (□) and (■), conversion, for the T and N samples, respectively.

riod (10 h) with smaller range of improvement (from 66 initially to 85% at steady state).

For the T-0.5 catalyst, increasing the reduction temperature to 623 K decreased by half the time required to achieve steady state; however, the steady-state selectivity was similar to that obtained after reduction at 493 K (88 and 91% for the 493 and 623 K reductions, respectively). For the N-0.5 sample, reduction at 623 K rather than 493 K did not significantly affect the time necessary to achieve steady state. But, the selectivity toward ethylene was only 75%, whereas it was 85% after reduction at 493 K. The TOF values, which were ca. 15% less for the N-0.5 sample than for the T-0.5 sample, were unaffected by the reduction temperature.

3.3. ^{119}Sn Mössbauer spectroscopy

The ^{119}Sn Mössbauer study was performed with the N-0.5 and T-0.5 catalysts, which have the same overall composition but were prepared by different methods. The spectra are shown in Fig. 3, and the parameters of the spectra are summarized in Table 3.

The Mössbauer spectrum of the as-prepared impregnated sample (T-0.5) consisted of a quadrupole doublet with a splitting of 0.50 $\mathrm{mm\,s^{-1}}$ and an isomer shift (IS) of 0.07 $\mathrm{mm\,s^{-1}}$ (Table 3). These parameters are characteristic of Sn^{4+} with Cl and O ligands [54]. Thus, even though the Sn precursor used to prepare the catalyst was $SnCl_2$, the Sn^{2+} oxidized to Sn^{4+} during storage of the catalysts, which is expected from the chemistry of Sn^{2+} compounds [55].

The spectrum of the as-prepared CSR sample (N-0.5) consisted of a quadrupole doublet of Sn^{4+} ($\mathrm{IS} = 0.02\ \mathrm{mm\,s^{-1}}$ and $\mathrm{QS} = 0.64\ \mathrm{mm\,s^{-1}}$) and a singlet with an IS of 1.63 $\mathrm{mm\,s^{-1}}$. The latter value is close to that of a Pt_3Sn alloy (1.50 $\mathrm{mm\,s^{-1}}$ [56]). Apparently alloying between Pt and Sn occurs under the conditions used to decompose the surface $Pt–Sn(C_2H_5)_{4-x}$ complex (Eqs. (2) and (3)). Whereas the Pt_3Sn alloy is stable during catalyst storage and/or exposure to air, the Sn-rich Pt–Sn alloy phase oxidizes into Sn^{4+}.

A characteristic feature of the reduced CSR sample (N-0.5) is the absence of ionic Sn species; the spectra contain only bands characteristic of Pt–Sn alloys (Fig. 3A, Table 3). However, the features of the Mössbauer spectra of the reduced impregnated catalyst (T-0.5) suggest the presence of three forms of Sn: Sn^{4+} species ($\mathrm{IS} = 0.38–0.54\ \mathrm{mm\,s^{-1}}$), Sn^{2+} species ($\mathrm{IS} = 3.95–4.15\ \mathrm{mm\,s^{-1}}$), and Pt–Sn alloys ($\mathrm{IS} = 1.11–2.53\ \mathrm{mm\,s^{-1}}$) [35,37,39,40,56], with a significant fraction of Sn alloyed with Pt (Table 3). The Sn^{2+} Mössbauer parameters were almost independent of the catalyst pretreatment and coincided with those for $SnCl_2$ [57]. The variation in the IS of the Sn^{4+} species for the reduced samples suggests that the environment of the Sn^{4+} ions depends on the reduction temperature [54,57]. Quadrupole splitting (QS) was not constrained for the Sn^{4+} species during deconvolution of the spectra. The QS of $SnCl_4$ is zero [57], and for SnO_2 it is 0.5–0.7 $\mathrm{mm\,s^{-1}}$ [35–37], a value very close to the line width of the ^{119}Sn source (0.63 $\mathrm{mm\,s^{-1}}$ [57]). Thus, when the relative intensity of the Sn^{4+} band was less than 20–30%, including a QS parameter did not increase the quality of the fit.

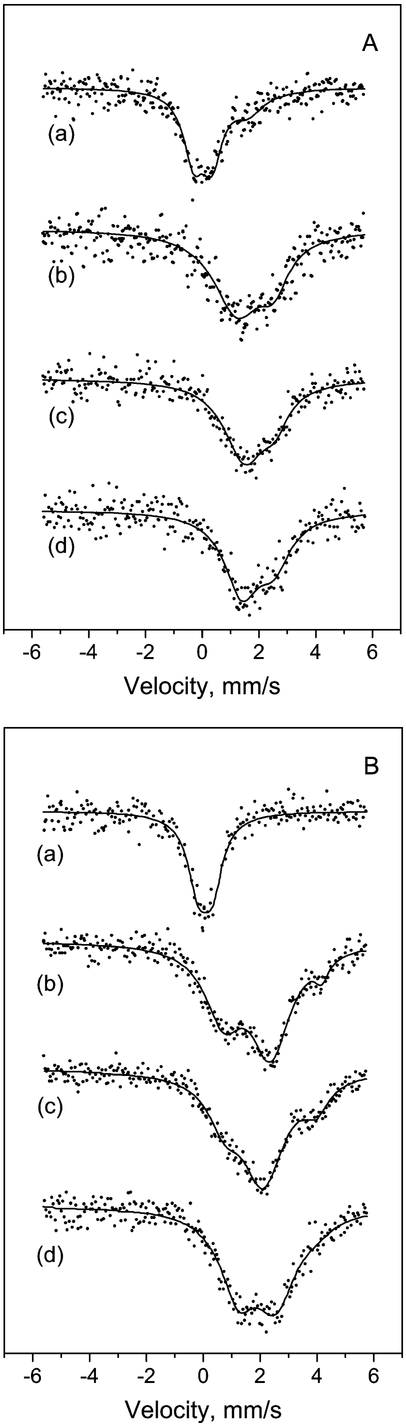

Fig. 3. Mössbauer spectra of the CSR (N-0.5) (A) and impregnated (T-0.5) (B) catalysts: (a) as prepared; (b) sample (a) after reduction with H_2 at 493 K for 2 h; (c) sample (b) after reduction with H_2 at 623 K for 2 h; (d) sample (c) after exposure to a flow of $CH_2Cl–CH_2Cl + H_2 + N_2$ (1:5:25) at 473 K for 24 h.

As already mentioned, the broad band in the range of 1–3 $\mathrm{mm\,s^{-1}}$ indicates that both the T-0.5 and the N-0.5 cata-

Table 3
Parameters of Mössbauer spectra of the Pt–Sn/SiO$_2$ catalysts

Sample	Treatment[a]	Species[b]	IS[c] (mm s^{-1})	QS[d] (mm s^{-1})	FWHM[e]	RI[f,g] (%)	S_{tot}[h] (a.u.)
T-0.5	As prepared[i]	Sn^{4+}	0.07	0.50	0.89	100	1.00
	Reduced by	Sn^{4+}	0.54	–	1.31	24	1.54
	H$_2$ at 493 K	Pt–Sn(a)	1.39	–	1.64	21	
		Pt–Sn(b)	2.45	–	1.48	50	
		Sn^{2+}	4.15	–	0.74	5	
	Reduced by	Sn^{4+}	0.38	–	0.68	6	1.74
	H$_2$ at 623 K	Pt–Sn(a)	1.11	–	1.29	19	
		Pt–Sn(b)	2.16	–	1.69	64	
		Sn^{2+}	3.95	–	1.14	12	
	Exposed to reaction	Pt–Sn(a)	1.22	–	1.59	43	1.42
	mixture at 473 K	Pt–Sn(b)	2.53	–	1.76	52	
		Sn^{2+}	3.96	–	1.58	5	
N-0.5	As prepared[i]	Sn^{4+}	0.02	0.64	0.88	79	1.00
		Pt–Sn(a)	1.63	–	1.36	21	
	Reduced by	Pt–Sn(a)	1.23	–	2.06	75	1.14
	H$_2$ at 493 K	Pt–Sn(b)	2.51	–	1.30	25	
	Reduced by	Pt–Sn(a)	1.51	–	1.80	80	1.09
	H$_2$ at 623 K	Pt–Sn(b)	2.58	–	1.17	20	
	Exposed to reaction	Pt–Sn(a)	1.38	–	1.49	63	0.94
	mixture at 473 K	Pt–Sn(b)	2.52	–	1.45	37	

[a] All experiments for a given catalyst were performed with the same sample that was treated in situ with H$_2$ first at 493 K for 2 h, then at 623 K for 2 h, and finally exposed to the CH$_2$Cl–CH$_2$Cl + H$_2$ + N$_2$ (1:5:25) flow at 473 K for 24 h.

[b] Pt–Sn(a), platinum-rich Pt–Sn alloys; Pt–Sn(b), tin-rich Pt–Sn alloys.

[c] Isomer shift relative to SnO$_2$.

[d] Quadrupole splitting.

[e] Full width at half maximum.

[f] Normalized relative intensity.

[g] Because the probability of the Mössbauer effect (recoilless fraction) is different for the various Sn species [57], the RIs do not strictly correspond to concentrations.

[h] The total spectral area related to the baseline, arbitrary units.

[i] Catalysts were stored in air.

lyst contained several Pt–Sn alloy phases (Fig. 3). The Mössbauer spectra were fit under the assumption of a two-alloy component system: a Pt-rich alloy (Pt–Sn(a)) with an IS of 1.1 to 1.7 mm s^{-1} and a Sn-rich alloy (Pt–Sn(b)) with an IS of 2.1 to 2.6 mm s^{-1}. The compositional changes in the Pt–Sn alloy species were estimated from the IS value with the assumption of proportionality between the IS and the Pt/Sn atomic ratio [56].

The changes in relative intensities (RIs) of the spectral components corresponding to the different Sn species and the changes in the composition of Pt–Sn alloys that resulted from different pretreatments for the T-0.5 and N-0.5 catalysts are described below. The RIs do not strictly correspond to concentration because the probability of the Mössbauer effect (recoilless fraction) varies with type of Sn species [57, 58]. In general, recoilless fractions for inorganic Sn^{2+} and Sn^{4+} compounds are less than those for Pt–Sn alloys [58, 59]. Thus, the relative concentrations of ionic Sn species determined solely from the RIs would be underestimated, and those of Pt–Sn alloy species would be overestimated. The total spectral area relative to the base line for the impregnated catalyst (T-0.5) increased significantly after each reduction and after exposure to the reaction mixture (Table 3). This increase may be associated with agglomeration of the Sn^{4+} at elevated temperatures as the recoilless fraction for bulk SnO$_2$ is larger than that for the surface Sn^{4+} ions [6]. The total spectral area for the CSR catalyst (N-0.5) was independent of the catalyst pretreatment, probably because Sn^{4+} moieties were absent in the reduced samples prepared by CSR.

For the Pt–Sn/SiO$_2$ catalyst prepared by co-impregnation (T-0.5), the IS and RI values were similar for the Sn-rich Pt–Sn alloy phase after reduction of the catalyst at 493 K and after exposure to the reaction mixture. Each IS of the alloy after these treatments exceeded that for the PtSn$_4$ phase (2.29 mm s^{-1} [56]). Reduction at 623 K resulted in a 13% higher RI and a lower IS (2.16 mm s^{-1}, which corresponds to the PtSn$_2$ phase [56]). A similar trend was observed for the Pt-rich Pt–Sn alloy phase—increasing the reduction temperature from 493 to 623 K decreased the IS from 1.39 to 1.11 mm s^{-1}. The IS increased to 1.22 mm s^{-1} after the reduced catalyst was exposed to the reaction mixture. (Isomer shifts below 1.40 mm s^{-1} correspond to diluted solutions of Sn in Pt [56].) In addition, exposure of the catalyst to the reaction mixture doubled the RI of the Pt-rich Pt–Sn alloy phase with respect to the value measured after the two reductions (from ca. 20 to 43%). When the reduction temperature was increased from 473 to 623 K, the RI of the band corresponding to ionic tin decreased from 29 to 18%. And then it decreased to 5% after exposure to the reaction mixture.

For the Pt–Sn/SiO_2 catalyst prepared by controlled surface reaction (N-0.5), the IS for the Sn-rich alloy phase was almost independent of the type of treatments: reduction at 493 K, reduction at 623 K, and exposure to the reaction mixture at 473 K (Table 3). Similar to the T-0.5 catalyst, the IS of the alloy after these treatments exceeded that of $PtSn_4$ [56]. The relative intensity of the band for the Sn-rich alloy phase decreased from 25 to 20% when the catalyst reduction temperature was increased from 493 to 623 K. But, exposure to the reaction mixture resulted in an increase in the RI of the Sn-rich alloy band to 37%. Correspondingly, the relative band intensity for the Pt-rich alloy phase increased with increasing catalyst reduction temperature, but it decreased after exposure of the reduced catalyst to the reaction mixture at 493 K. The IS values of the Pt-rich phase after reduction at 493 K and exposure to the reaction mixture at 473 K (1.23–1.38 $mm\,s^{-1}$, Table 3) are indicative of a low concentration ($<$ 6 at%) of metallic tin dissolved in Pt. However, after reduction at 623 K the IS of the Pt-rich phase (1.51 $mm\,s^{-1}$) corresponded to the Pt_3Sn stoichiometry [56].

4. Discussion

The positive effect of Sn addition on the performance of Pt hydrocarbon reforming catalysts has fueled debates about the appropriate molecular-level description to account for the role of Sn [1,2]. Both Sn^{n+} ($n = 2, 4$) species and metallic Sn alloyed with Pt have been suggested to be responsible for the improvement of the catalytic properties of Pt. For Sn^{n+} a mechanism was proposed in which there is an electronic interaction between highly dispersed Pt particles and Sn ions bound to the support [60–63]. For metallic Sn alloyed with Pt, it was proposed that the Sn atoms serve as spacers that split the Pt ensembles and thereby suppress the size-demanding reactions such as hydrogenolysis; thus, the role of Sn in this case is viewed as entirely geometric [29,64,65]. Electronic modification of Pt alloyed with Sn was found to be insignificant [1,65–67], although theoretical consideration of the Pt–Sn bonding in Pt–Sn surface alloys suggests a $Sn(5s, 5p) \rightarrow Pt(6s, 6p)$ charge transfer and a $Pt(5d) \rightarrow Pt(6s, 6p)$ rehybridization that localize electrons between the metal centers [68,69].

The exceptional performance of Pt–Sn catalysts in reactions such as the activation of C=O bonds (CO oxidation [5–7], olefin hydroformylation [14], selective hydrogenation of α, β-unsaturated aldehydes [16–20]) stimulated further discussion about the mechanism by which Sn modifies the catalytic performance of Pt. It was proposed that the Sn ions of Pt–Sn^{n+} sites interact as a Lewis acid with the oxygen atom of the C=O bond, thereby activating the carbonyl group [25]. The Sn ions that strongly interact with the support are always present in reduced catalysts prepared by impregnation [6,21,27,35–37,39,70–75]. Some of them may be located at the Pt-support interface to form the Pt–Sn^{n+} moieties. For the Pt–Sn catalysts prepared by the controlled surface reaction method in which all Sn is deposited on the surface of Pt particles and reduces to Sn^0, it was proposed that partially polarized species such as $Pt^{\delta-}$–$Sn^{\delta+}$ serve as active sites for reactions of carbonyl compounds [25]. However, it was also shown that Sn^{n+} species are present in reduced "organometallic" catalysts [6,20,76,77]. Furthermore, a fraction of Sn on the surface of Pt–Sn alloys is oxidized by the $CO + O_2$ reaction mixture in the case of CO oxidation [6,43] or by the α, β-unsaturated aldehyde in the case of aldehyde hydrogenation [78]. The participation of Sn^{n+} ions in CO bond activation results in an increase in the reaction rate for CO oxidation reaction [5–7]; for α, β-unsaturated aldehyde hydrogenation the presence of Sn^{n+} ions in the Pt–Sn catalyst improves the selectivity toward α, β-unsaturated alcohols (C=O bond hydrogenation) as opposed to saturated aldehydes (C=C bond hydrogenation) [17–20].

A mechanism similar to the activation of the C=O group of carbonyl compounds appears to be appropriate for the activation of C–Cl bonds. The interaction of Cl atoms (Lewis bases) of 1,2-dichloroethane with Sn^{2+} ions (Lewis acids) weakens both C–Cl bonds of a vicinal halocarbon to favor bond dissociation:

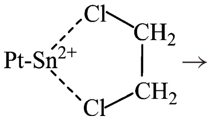

$$\rightarrow Pt\text{–}Sn^{4+}Cl_2 + CH_2{=}CH_2, \quad (4)$$

$$Pt\text{–}Sn^{4+}Cl_2 + 2H_{ads} \rightarrow Pt\text{–}Sn^{2+} + 2HCl.$$

The two C–Cl bonds of the 1,2-dichloroethane molecule dissociate, which results in the formation of ethylene and the oxidation of the Sn^{2+} ion to Sn^{4+}. As ethylene does not interact strongly with Sn^{n+} ions (as well as with Sn metal), it immediately desorbs into the gas phase. The dissociation of H_2 occurs on the Pt sites. And the H atoms diffuse from Pt sites to reduce the Sn^{4+} to Sn^{2+} to complete the catalytic cycle. In fact, intimate contact between Pt and Sn^{n+} ions is not required because spillover provides the flux of H atoms necessary to reduce the Sn^{4+} ions. However, the dissociation of C–Cl bonds also occurs on Sn^0 [79]. If the Sn^0 species participate as sites for C–Cl bond dissociation, a mechanistic scheme for the dechlorination reaction could be written as follows:

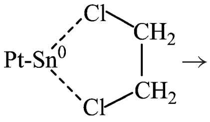

$$\rightarrow Pt\text{–}Sn^{2+}Cl_2 + CH_2{=}CH_2, \quad (5)$$

$$Pt\text{–}Sn^{2+}Cl_2 + 2H_{ads} \rightarrow Pt\text{–}Sn^0 + 2HCl.$$

If 1,2-dichloroethane dissociates on Pt sites, ethane forms as a reaction product [80]. Ethylene adsorbs strongly on Pt [81–83] and is hydrogenated to ethane rather than desorbs as ethylene.

A comparison of the catalytic performances of the two Pt–Sn/SiO_2 catalysts with the same overall composition but prepared differently provides insight into the viability of the reaction mechanisms shown schematically by Eqs. (4) and (5).

A characteristic performance feature of the co-impregnation catalyst (T-0.5) is the transient period in terms of ethylene selectivity (Table 2, Fig. 2). At early time on stream, the catalyst exhibits relatively low selectivity toward ethylene, which increases substantially during the course of the reaction. The Mössbauer results show that a significant fraction of Sn in the reduced catalyst incorporates into a Pt–Sn alloy with a $Pt_\infty Sn$ stoichiometry (diluted solid solution of Sn in Pt) (Table 3). Similar to pure Pt, the $Pt_\infty Sn$ alloy catalyzes 1,2-dichloroethane dechlorination to form ethane, whereas the Sn-rich Pt–Sn alloy is responsible for the ethylene formation [21]. The fraction of Sn in the $Pt_\infty Sn$ alloy increases after 24 h on stream (Table 3), in parallel with an increase in the ethylene selectivity (Fig. 3, Table 3). This indicates that the relative impact of the $Pt_\infty Sn$ phase in the impregnated catalyst (T-0.5) on the catalytic performance decreases with time on stream.

The inhomogeneity of supported bimetallic catalysts prepared by co-impregnation [36,41] allows for the possibility that the reduced catalyst contains a fraction of unalloyed Pt (or PtSn particles with very low Sn concentration) in addition to the Pt–Sn alloy species. As the dechlorination reaction proceeds, the Pt alloys with Sn that remained in an oxidized state after catalyst reduction to increase the concentration of Sn in both the $Pt_\infty Sn$ and Sn-rich Pt–Sn alloy (the IS of both the Pt–Sn(a) and Pt–Sn(b) species is greater after exposure of the catalyst to reaction mixture than after reduction at 623 K (Table 3)). Table 3 shows that the fraction of ionic Sn does indeed decrease after the reduced catalyst is exposed to the reaction mixture. As alloying of a Pt–Sn particle with the additional Sn starts from the surface, the concentration of Sn on the surface of the particle can be significantly higher than the Sn concentration in the bulk of the particle.

There is also the possibility of a “true” surface enrichment in Sn that should be more pronounced for the Pt-rich Pt–Sn species. This enrichment occurs at the expense of the bulk Sn concentration and is enhanced by exposure to the reaction mixture. Surface segregation of alloys during exposure to different gaseous media is not uncommon [84,85]. Indeed, surface enrichment in Sn of the outermost surface layers of bulk Pt–Sn alloys has been demonstrated [86–89]. The driving force for surface enrichment of Pt–Sn alloys in Sn during the dechlorination reaction is the difference in affinity of Pt and Sn toward Cl. Specifically, $\Delta H_\mathrm{f}^\mathrm{o}$ is $-325\ \mathrm{kJ\,mol^{-1}}$ for $SnCl_2$ and $-123\ \mathrm{kJ\,mol^{-1}}$ for $PtCl_2$ [90]. Thus, the alloying of an additional amount of Sn with Pt–Sn species during the dechlorination reaction and surface enrichment in Sn explain the transient behavior of the impregnated T-0.5 catalyst with respect to ethylene selectivity (Fig. 3); the ethylene selectivity increases with increasing surface concentration of Sn.

The samples prepared by CSR (N-series) also exhibit transient behavior during the $CH_2Cl–CH_2Cl + H_2$ reaction (Figs. 1 and 2; Table 2), although the magnitude of the selectivity change with time on stream is much lower than for the impregnated catalysts. Preparation by controlled surface reaction ensures exclusive interaction of $Sn(C_2H_5)_4$ with Pt particles [19,45,47,91]. Indirect evidence that all Sn in the “organometallic” catalysts interacts with Pt is provided by the Mössbauer results, showing that the reduced CSR sample (N-0.5) does not contain ionic Sn (Table 3). Thus, the increase in ethylene selectivity with time on stream for the CSR samples cannot be explained by the same mechanism as that for the impregnated T-0.5 sample in which the fraction of Sn that remained in the oxidized state after catalyst reduction reduces to the metal during the dechlorination reaction and alloys with Pt to increase the Sn/Pt atomic ratio in the bimetallic particles and, hence, the ethylene selectivity.

The essence of the CSR technique is that the Sn organic moieties are deposited on the surface of Pt particles layer by layer [45]. The number of the layers is not a function of the Pt particle size. (Metal particles in supported catalysts are always inhomogeneous with regard to size.) And, therefore, the Sn/Pt atomic ratio for smaller particles will be higher than that for larger particles. During decomposition of the surface Pt–Sn complex, Sn atoms “sink” in the bulk of the Pt particles to form Pt–Sn alloys. Thus, the particles with a lower Sn/Pt atomic ratio have a lower Sn concentration on the surface, and these particles catalyze 1,2-dichloroethane dechlorination to ethane. Exposure of the reduced catalyst to the reaction mixture triggers the process of surface enrichment in Sn, and ethylene selectivity increases. However, there may be particles that do not have enough Sn to turn into ethylene-selective entities, even though all of the Sn accumulates on the particle surface. Ultimately, the ongoing surface enrichment in Sn leads to “cherry-like” particles with Pt-rich Pt–Sn alloy or even a monometallic Pt core surrounded by Sn-rich Pt–Sn alloy.

A higher reduction temperature or a longer reduction time at a fixed temperature favors more homogeneous Pt–Sn particles with respect to the Sn and Pt distribution in the particle bulk. But, reduction with H_2 favors surface enrichment of bimetallic Pt–Sn particles in Pt [77]. Thus, the lower ethylene selectivity of the CSR N-0.5 sample after reduction at 623 K than after reduction at 493 K (Fig. 2) can be attributed to the higher surface concentration of Pt after the reduction at a higher temperature. If diffusion of Sn and Pt in the Pt–Sn alloys is slow, a longer time is required for the bimetallic particles to equilibrate with the reaction mixture with respect to surface Sn concentration at the reaction temperature (473 K).

For the impregnated samples the diffusion of Sn into bulk during high temperature reduction does not affect the surface concentration of Sn as significantly as it does for the CSR samples. About 30% of the Sn in the impregnated T-0.5 sample reduced at 493 K exists as Sn^{n+} ions with O and/or Cl ligands (Table 3). These Sn moieties must be located sufficiently far from the Pt-containing particles that reduction to Sn and incorporation into a Pt–Sn alloy do not occur during the limited time of reduction. Increasing the reduction temperature to 623 K results in a decrease in the Sn^{n+} species concentration from ~ 30 to $\sim 20\%$. Hence, the decrease in the concentration of Sn on the surface of Pt–Sn particles during catalyst reduction due to diffusion of Sn into the bulk is compensated for by a supply of additional Sn (that has been located on the support as Sn^{n+} ions) to the particle surface. The fact that the concentration of ionic Sn decreases during the dechlorination reaction from 18 to 5% after 24 h on stream (Table 3) provides evidence that there is a flux of Sn toward the Pt–Sn alloy particles during the dechlorination reaction. Thus, the concentration of Sn on the surface of Pt–Sn particles is higher for the impregnated catalyst than for the CSR sample; this accounts for the higher steady-state ethylene selectivity of the T-0.5 sample than the N-0.5 catalyst (Fig. 3, Table 2).

The catalytic tests show that the activities of the impregnated (T-0.5) and CSR (N-0.5) samples in the 1,2-dichloroethane dechlorination reaction are the same within experimental error (Table 2). The absence of ionic Sn species in the CSR (N-0.5) sample exposed to the $CH_2Cl–CH_2Cl + H_2$ reaction mixture (Table 3) suggests that Sn^{2+} ions are not active species for 1,2-dichloroethane dechlorination, according to Eq. (4). If they were, the activity of the impregnated sample would be higher because the concentration of the Sn^{2+} ions after exposure to the reaction mixture is significant (5%, Table 3). Typically, the steady-state concentration of a reaction intermediate under conditions of real catalysis is low, and it is difficult to detect the intermediate by conventional characterization techniques. The fact that the Sn^{2+} species were identified for the impregnated (T-0.5) sample exposed to the reaction mixture suggests that these moieties are spectator species, most likely located far from the Pt-containing particles that dissociate H_2. The presence of Sn^{2+} ions in the impregnated (T-0.5) sample would account for the higher concentration of Cl in the used impregnated sample than in the used CSR sample (Table 1), because Cl may serve as a ligand for ionic Sn species.

5. Conclusion

For the reaction of hydrogen-assisted 1,2-dichloroethane dechlorination, the catalytic performance of $Pt–Sn/SiO_2$ catalysts with different Pt/Sn atomic ratios prepared by controlled surface reaction with an organometallic Sn precursor has been compared with that of a $Pt–Sn/SiO_2$ catalyst prepared by co-impregnation. The application of controlled surface reaction technique to prepare $Pt–Sn/SiO_2$ catalysts results in the exclusive formation of Pt–Sn bimetallic surface entities. Conversely, the co-impregnation preparation technique results in the stabilization of Sn^{2+} and Sn^{4+} moieties on the support surface in addition to the formation of Pt–Sn alloys. Independent of the catalyst preparation method, the catalytic activity decreases with an increase in the Sn concentration, but it is approximately the same for catalysts with the same Pt/Sn atomic ratio.

Both the CSR and the impregnated catalysts with a Pt/Sn atomic ratio less than unity exhibit high steady-state selectivity toward ethylene; however, the selectivity typically increases with time on stream. The most dramatic selectivity increase was observed for the co-impregnated $Pt–Sn/SiO_2$ catalysts. Specifically, the ethylene selectivity for the catalyst with a Pt/Sn atomic ratio of 0.5 was 5% initially but increased to 91% in 35 h on stream. The transient behavior of the "organometallic" catalysts is explained by Sn enrichment of the Pt–Sn particle surface during the course of the dechlorination reaction, as Sn-rich Pt–Sn alloys are highly selective toward ethylene. The surface of Pt–Sn particles of the co-impregnated $Pt–Sn/SiO_2$ catalysts is also enriched in Sn during the 1,2-dechlorination reaction, resulting in an increase in the ethylene selectivity; however, the enrichment occurs during the dechlorination reaction by incorporation of an additional amount of Sn that was present on the support in an oxidized state before the start of the reaction.

A mechanism of hydrogen-assisted 1,2-dichloroethane dechlorination catalyzed by $Pt–Sn/SiO_2$ was proposed. It consists of dissociation of both C–Cl bonds of the 1,2-dichloroethane molecule on a Sn atom incorporated into a Pt–Sn alloy. The dissociation results in the formation of an ethylene molecule and oxidation of Sn^0 to Sn^{2+}. Reduction of the Sn^{2+} ion with H atoms diffused from Pt to form Sn^0 and HCl regenerates the active site, thereby completing the catalytic cycle.

Acknowledgment

Financial support from the Department of Energy–Basic Energy Sciences (DE-FG02-95ER14539) is gratefully acknowledged.

References

[1] V. Ponec, Adv. Catal. 32 (1983) 149.

[2] J.H. Sinfelt, Bimetallic Catalysts: Discoveries, Concepts, and Application, Wiley, New York, 1983.

[3] P. Chantaravitoon, S. Chavadej, J. Schwank, Chem. Eng. J. 97 (2004) 161.

[4] I. Honma, T. Toda, J. Electrochem. Soc. 150 (2003) A1689.

[5] J. Margitfalvi, I. Borbáth, M. Hegedüs, A. Szegedi, K. Lázár, S. Göbölös, S. Kristyán, Catal. Today 73 (2002) 343.

[6] K. Lázár, W.D. Rhodes, I. Borbáth, M. Hegedüs, J.L. Margitfalvi, Hyperfine Interactions 139/140 (2002) 87.
[7] J. Margitfalvi, I. Borbáth, M. Hegedüs, E. Tfirst, S. Göbölös, K. Lázár, J. Catal. 196 (2000) 200.
[8] S.N. Pavlova, V.A. Sadykov, Yu.V. Frolova, N.F. Saputina, P.M. Vedenkin, I.A. Zolotarskii, V.A. Kuzmin, Chem. Eng. J. 91 (2003) 227.
[9] J. Salmones, J.-A. Wang, J.A. Galicia, G. Aguilar-Rios, J. Mol. Catal A 184 (2002) 203.
[10] C. Yokoyama, S.S. Bharadwaj, S.S.L.D. Schmidt, Catal. Lett. 38 (1996) 181.
[11] O.A. Bariås, A. Holmen, E.A. Blekkan, J. Catal. 158 (1996) 1.
[12] G. Corro, J.L.G. Fierro, R. Montiel, S. Castillo, M. Moran, Appl. Catal. B 46 (2003) 307.
[13] G. Corro, R. Montiel, J. Mol. Catal. A 184 (2002) 443.
[14] A. Marteel, J.A. Davies, M.R. Mason, T. Tack, S. Bektesevich, M.A. Abraham, Catal. Commun. 4 (2003) 309.
[15] S. Göbölös, N. Mahata, I. Borbáth, M. Hegedüs, J.L. Margitfalvi, React. Kinet. Catal. Lett. 74 (2001) 345.
[16] J.M. Ramallo-López, G.F. Santori, L. Giovanetti, M.L. Casella, O.A. Ferretti, F.G. Requejo, J. Phys. Chem. B 107 (2003) 11441.
[17] G.F. Santori, M.F. Cazella, O.A. Ferretti, J. Mol. Catal. A 186 (2002) 223.
[18] G.F. Santori, M.F. Cazella, G.J. Siri, H.R. Aduriz, O.A. Ferretti, React. Kinet. Catal. Lett.75 (2002) 225.
[19] J.L. Margitfalvi, I. Borbáth, M. Hegedüs, A. Tompos, Appl. Catal. A 229 (2002) 35.
[20] L. Stievano, F.E. Wagner, S. Calogero, S. Recchia, C. Dossi, R. Psaro, Stud. Surf. Sci. Catal. 130 (2000) 3903.
[21] W.D. Rhodes, K. Lázár, V.I. Kovalchuk, J.L. d'Itri, J. Catal. 211 (2002) 173.
[22] K. Early, W.D. Rhodes, V.I. Kovalchuk, J.L. d'Itri, Appl. Catal. B 26 (2000) 257.
[23] F. Delbecq, P. Sautet, J. Catal. 220 (2003) 115.
[24] D.I. Jerdev, A. Olivas, B.E. Koel, J. Catal. 205 (2002) 278.
[25] P. Claus, Top. Catal. 5 (1998) 51.
[26] P. Biloen, J.N. Helle, H. Verbeek, F.M. Dautzenburg, W.H.M. Sachtler, J. Catal. 63 (1980) 112.
[27] G. Meitzner, G.H. Via, F.W. Lytle, S.C. Fung, J.H. Sinfelt, J. Phys. Chem. 92 (1988) 2925.
[28] H. Verbeek, W.M.H. Sachtler, J. Catal. 42 (1976) 257.
[29] Y.X. Li, K.J. Klabunde, J. Catal. 126 (1990) 173.
[30] R. Burch, L.C. Garla, J. Catal. 71 (1981) 360.
[31] R. Burch, J. Catal. 71 (1981) 348.
[32] O.A. Bariås, A. Holmen, E.A. Blekkan, Catal. Today 24 (1995) 361.
[33] A. Palazov, Ch. Bonev, D. Shopov, G. Lietz, A. Sárkány, J. Völter, J. Catal. 103 (1987) 249.
[34] T.B. Massalski, H. Okamoto, P.R. Subramanian, L. Kacprzak (Eds.), Binary Alloy Phase Diagrams, ASM International, 1990.
[35] R. Bacaud, P. Bussière, F. Figueras, J. Catal. 69 (1981) 399.
[36] V.I. Kuznetsov, A.S. Belyi, E.M. Yurchenko, M.D. Smolikov, M.T. Protasova, E.V. Zatolokina, V.K. Duplyakin, J. Catal. 99 (1986) 159.
[37] Y.-X. Li, K.J. Klabunde, B.H. Davis, J. Catal. 128 (1991) 1.
[38] T.P. Chojnacki, L.D. Schmidt, J. Catal. 129 (1991) 473.
[39] M.C. Hobson Jr., S.L. Goresh, G.P. Khare, J. Catal. 142 (1993) 641.
[40] C. Kappenstein, M. Guérin, K. Lázár, K. Matusek, Z. Paál, J. Chem. Soc., Faraday Trans. 94 (1998) 2463.
[41] J.J. Burton, R.L. Garten, in: J.J. Burton, R.L. Garten (Eds.), Advanced Materials in Catalysis, Academic Press, New York, 1977, p. 33.
[42] Yu.I. Yermakov, B.N. Kuznetsov, V.I. Zakharov, Catalysis by Supported Complexes, Elsevier, Amsterdam, 1981.
[43] J.L. Margitfalvi, I. Borbáth, K. Lázár, E. Tfirst, A. Szegedi, M. Hegedüs, S. Göbölös, J. Catal. 203 (2001) 94.
[44] J.L. Margitfalvi, E. Tálas, S. Göbölös, Catal. Today 6 (1989) 73.
[45] J.L. Margitfalvi, I. Borbáth, E. Tfirst, A. Tompos, Catal. Today 43 (1998) 29.
[46] J.L. Margitfalvi, I. Borbáth, M. Hegedüs, S. Göbölös, F. Lónyi, React. Kinet. Catal. Lett. 68 (1999) 133.
[47] J.L. Margitfalvi, I. Borbáth, J. Mol. Catal. A 202 (2003) 313.
[48] J.P. Candy, B. Didillon, E.L. Smith, T.B. Shay, J.M. Basset, J. Mol. Catal. 86 (1994) 179.
[49] J.L. Margitfalvi, M. Hegedüs, S. Göbölös, E. Kern-Tálas, P. Szedlacsek, S. Szabó, F. Nagy, in: Proceedings of the 8th International Congress on Catalysis, vol. 4, Chemie, Weinheim, 1985, p. 903.
[50] E. Kern-Tálas, M. Hegedüs, S. Göbölös, P. Szedlacsek, J.L. Margitfalvi, Stud. Surf. Sci. Catal. 31 (1987) 689.
[51] P.A. Webb, C. Orr, Analytical Methods in Fine Particle Technology, Micromeritics Instrument Corporation, Norcross, GA, 1997.
[52] K. Lázár, Struct. Chem. 2 (1991) 245.
[53] L.S. Vadlamannati, D.R. Luebke, V.I. Kovalchuk, J.L. d'Itri, Stud. Surf. Sci. Catal. 130 (2000) 233.
[54] R.V. Parish, in: G.J. Long (Ed.), in: Mössbauer Spectroscopy Applied to Inorganic Chemistry, vol. 1, Plenum, New York, 1984, p. 527.
[55] F.A. Cotton, G. Wilkinson, Advanced Inorganic Chemistry, Wiley, New York, 1988.
[56] J.S. Charlton, M. Cordey-Hayes, I.R. Harris, J. Less-Common Met. 20 (1970) 105.
[57] N.N. Greenwood, T.C. Gibb, Mössbauer Spectroscopy, Chapman–Hall, London, 1971.
[58] M.C. Hayes, in: V.I. Goldanskii, R.H. Herber (Eds.), Chemical Applications of Mössbauer Spectroscopy, Academic Press, New York, 1968, p. 314.
[59] V.A. Bryukhanov, N.N. Delyagin, R.N. Kuz'min, V.S. Shpinel', Soviet Phys. JETP 19 (1964) 1344.
[60] P.A. Zhdan, B.N. Kuznetsov, A.P. Shepelin, V.I. Kovalchuk, Yu.I. Yermakov, React. Kinet. Catal. Lett. 18 (1981) 267.
[61] B.N. Kuznetsov, V.K. Duplyakin, V.I. Koval'chuk, Yu.I. Ryndin, A.S. Belyi, Kinet. Catal. 22 (1982) 1183.
[62] A.P. Shepelin, A.P. Chernyshov, V.I. Koval'chuk, P.A. Zhdan, E.N. Yurchenko, B.N. Kuznetsov, Yu.I. Yermakov, Kinet. Catal. 22 (1982) 548.
[63] Yu.A. Ryndin, J. Lorent, B.N. Kuznetsov, V.I. Kovalchuk, A. Pentenero, Yu.I. Yermakov, Kinet. Catal. 22 (1982) 513.
[64] B.H. Davis, J. Catal. 46 (1977) 348.
[65] F.B. Passos, M. Schmal, M.A. Vannice, J. Catal. 160 (1996) 106.
[66] A.G.T.M. Bastein, F.J.C.M. Toolenaar, V. Ponec, J. Catal. 90 (1984) 88.
[67] K. Balakrishnan, J. Schwank, J. Catal. 138 (1992) 491.
[68] J.A. Rodrigues, S. Chaturvedi, T. Jirsak, J. Hrbek, J. Chem. Phys. 109 (1998) 4052.
[69] J.A. Rodrigues, T. Jirsak, S. Chaturvedi, J. Hrbek, J. Am. Chem. Soc. 120 (1998) 11149.
[70] K. Balakrishnan, J. Schwank, J. Catal. 127 (1991) 287.
[71] B.E. Handy, J.A. Dumesic, R.D. Sherwood, R.T.K. Baker, J. Catal. 124 (1990) 160.
[72] B.A. Sexton, A.E. Hughes, K. Foger, J. Catal. 88 (1984) 466.
[73] S.R. Adkins, B.H. Davis, J. Catal. 89 (1994) 371.
[74] H. Lieske, J. Völter, J. Catal. 90 (1984) 96.
[75] A.C. Muller, P.A. Engelhard, J.E. Weisang, J. Catal. 56 (1979) 65.
[76] Cs. Vértes, E. Tálas, I. Czakó-Nagy, J. Ryczkowski, S. Göbölös, A. Vértes, J. Margitfalvi, Appl. Catal. 68 (1991) 149.
[77] E. Merlen, P. Beccat, J.C. Bertolini, P. Delichère, N. Zanier, B. Didillon, J. Catal. 159 (1996) 178.
[78] J. Margitfalvi, Gy. Vankó, I. Borbáth, A. Tompos, A. Vértes, J. Catal. 190 (2000) 474.
[79] Z. Hauptmann, J. Graefe, H. Remane, Lehrbuch der Organische Chemie, VEB Deutscher Verlag für Grundstoffindustrie, Leipzig, 1976.
[80] V.I. Kovalchuk, J.L. d'Itri, Appl. Catal. A 271 (2004) 13.
[81] J. Shen, J.M. Hill, R.M. Watwe, B.E. Spiewak, J.A. Dumesic, J. Phys. Chem. B 103 (1999) 3923.
[82] Y.-L. Tsai, C. Xu, B.E. Koel, Surf. Sci. 385 (1997) 37.

[83] M.T. Paffett, S.C. Gebhard, R.G. Windham, B.E. Koel, Surf. Sci. 223 (1989) 449.

[84] P. Bodnariuk, B. Coq, G. Ferrat, F. Figueras, J. Catal. 116 (1989) 459.

[85] V. Ponec, Catal. Rev.-Sci. Eng. 11 (1975) 41.

[86] R. Bouwman, P. Biloen, Surf. Sci. 41 (1974) 34.

[87] G.B. Hoflund, D.A. Asbury, P. Kirszensztejn, H.A. Laitenen, Surf. Interface Anal. 9 (1986) 169.

[88] G.B. Huflund, D.A. Asbury, P. Kirszensztejn, H.A. Laitenen, Surf. Sci. 161 (1985) L583.

[89] G.B. Huflund, D.A. Asbury, Langmuir 2 (1986) 695.

[90] CRC Handbook of Chemistry and Physics, 73rd ed., CRC Press, Boca Raton, 1992.

[91] J.L. Margitfalvi, I. Borbáth, A. Tompos, Stud. Surf. Sci. Catal. 118 (1998) 195.